

Q-Align: Alleviating Attention Leakage in Zero-Shot Appearance Transfer via Query-Query Alignment

Namu Kim^{*1}

namu.kim@kt.com

Wobin Kweon^{*2}

wonbin@illinois.edu

Minsoo Kim^{*3}

km19809@postech.ac.kr

Hwanjo Yu^{†3}

hwanjoyu@postech.ac.kr

¹ KT Corporation, South Korea² University of Illinois Urbana-Champaign, USA³ Pohang University of Science and Technology (POSTECH), South Korea

27 Aug 2025

arXiv:2508.21090v1 [cs.CV]

Abstract

We observe that zero-shot appearance transfer with large-scale image generation models faces a significant challenge: *Attention Leakage*. This challenge arises when the semantic mapping between two images is captured by the Query-Key alignment. To tackle this issue, we introduce **Q-Align**, utilizing Query-Query alignment to mitigate attention leakage and improve the semantic alignment in zero-shot appearance transfer. Q-Align incorporates three core contributions: (1) Query-Query alignment, facilitating the sophisticated spatial semantic mapping between two images; (2) Key-Value rearrangement, enhancing feature correspondence through realignment; and (3) Attention refinement using rearranged keys and values to maintain semantic consistency. We validate the effectiveness of Q-Align through extensive experiments and analysis, and Q-Align outperforms state-of-the-art methods in appearance fidelity while maintaining competitive structure preservation.

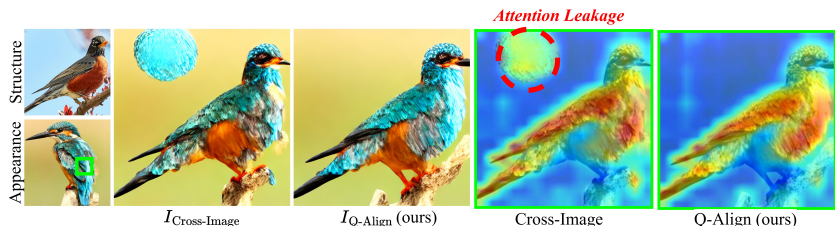


Figure 1: Attention leakage in Cross-Image [1]. The green-outlined images show the attention map corresponding to the bird's body (a green square in Appearance image).

© 2025. The copyright of this document resides with its authors.

It may be distributed unchanged freely in print or electronic forms.

^{*} These authors contributed equally to this work.

[†] Corresponding author.

1 Introduction

Appearance transfer is an image generation process where the structure image establishes the framework of semantic regions, and the appearance image provides the texture and identity details to fill those regions. As illustrated in Figure 1, for example, the wings in the appearance image are transferred to the wing regions of the structure image, branches to branches, and background to background. To achieve this, the primary challenge is achieving precise semantic alignment between the features of the two images.

Early methods relied on rule-based techniques [2, 23] for semantic correspondence, but were limited in their adaptability to diverse and complex datasets. With advances in deep learning, data-driven approaches [5, 10, 31, 32] were introduced to improve alignment accuracy. Although these methods demonstrated promising performance, they depend on ground-truth correspondence and require extensive labeled training datasets. Pre-trained vision transformer features [6, 11] have gained attention as a solution to overcome these limitations by enabling the extraction of correspondence maps without labeled datasets [12, 13].

More recently, large-scale image generation models [10, 27, 28] have introduced powerful generative capabilities that can be leveraged to discover semantic maps [13, 24, 30, 33] in a *zero-shot* manner. These models are utilized in various ways, such as using the generative model as an encoder to extract semantically aligned features [22, 25, 33] or through attention control [8, 14, 26, 27] to manipulate specific regions. Further research has analyzed the role of attention [21] and optimized its mechanisms [26] for improved performance.

The prominent method in zero-shot appearance transfer, Cross-Image [10], effectively performs appearance transfer without training by leveraging large-scale image generation models and employing attention control, based on MasaCtrl [8]. Despite its effectiveness, Cross-Image exhibits a significant challenge: *attention leakage*. We define the attention leakage as instances where the object(or background) is mapped to the background(or object), or the semantic mapping within the object itself is incorrect. As shown in Figure 1, attention to the bird’s body spills over to random background regions rather than remaining focused on the bird itself.

This paper proposes **Q-Align**, a novel approach for zero-shot appearance transfer that mitigates attention leakage without requiring any optimization process or additional data. We provide an in-depth analysis of attention leakage in Cross-Image and introduce a novel approach based on query-query alignment, as follows:

- We highlight our key observation that naive mixing of query, key, and value can cause misalignment between features, leading to attention leakage (Section 3).
- We demonstrate that query-query alignment offers more sophisticated spatial semantic mapping, and propose a key-value rearrangement technique to improve query-key-value correspondence in the conventional Cross-Image attention approach (Section 4).
- We validate the effectiveness of the proposed method through a novel evaluation protocol leveraging GPT-4o series, and provide a detailed analysis of each component (Section 5).

The official implementation of Q-Align is publicly available¹.

¹<https://github.com/SEED-TO-TREE/Q-Align-BMVC2025>

2 Preliminary

Problem Formulation. Given a pair of images, I_{app} and I_{str} , the appearance transfer task aims to generate I_{out} by transferring the appearance of I_{app} onto I_{str} , mapping semantically corresponding regions and ensuring coherence between objects and backgrounds. In Figure 1, features such as wings, beak, and branches in I_{app} should be aligned with semantically corresponding regions in I_{str} . Additionally, the background of I_{app} needs to be smoothly integrated into that of I_{str} , creating a cohesive and visually seamless result.

Cross-Image Attention. The cross-image attention mechanism [11] is built upon the mutual attention of MasaCtrl [8], which demonstrates how the appearance of input image can be semantically mapped to the structure of the output image. Since self-attention layers allow the model to capture feature correspondences within an image, the queries, keys, and values of these layers can also be leveraged to infer corresponding regions between different images. Let $(Q_{\text{app}}, K_{\text{app}}, V_{\text{app}})$ and $(Q_{\text{out}}, K_{\text{out}}, V_{\text{out}})$ denote the queries, keys, and values corresponding to I_{app} and I_{out} , respectively, within a specific self-attention layer. The cross-image attention is defined by replacing $K_{\text{out}}, V_{\text{out}}$ with $K_{\text{app}}, V_{\text{app}}$ as follows:

$$\text{softmax} \left(\frac{Q_{\text{out}} K_{\text{app}}^\top}{\sqrt{d}} \right) V_{\text{app}}. \quad (1)$$

Q_{out} determines the spatial semantics and is initialized as Q_{str} at the first diffusion step. K_{app} offers appearance context for each query. By doing so, Cross-Image enables the model to implicitly transfer the visual appearance between semantically similar objects in the different images.

3 Motivation

Attention Leakage. Figure 1 shows attention leakage in Cross-Image during the appearance transfer from I_{app} to I_{str} , causing unreliable generation in $I_{\text{Cross-Image}}$. To analyze the artifact in the upper left of $I_{\text{Cross-Image}}$, we examine the attention map for the bird’s body (green square) in I_{app} . The attention erroneously shifts to a background region instead of focusing on the bird (*i.e.*, it *leaks* into irrelevant areas). This misaligns the background and draws attention to unrelated features (*e.g.*, a mint-colored bird). In our experiment, attention leakage occurs in 94 of 180 pairs (52.2%), and Q-Align improves 65 of these (69.1%).

Query-Key Misalignment. Cross-Image relies solely on $Q_{\text{out}} K_{\text{app}}^\top$ to infer semantically corresponding regions between I_{out} and I_{app} , and faces the attention leakage. This issue arises when the attention mechanism fails to accurately attend to the corresponding regions, shifting instead to incorrect locations and generating erroneous images. We will discuss further on Query-Key misalignment with Figure 3 in the following section.

Naive Approaches. Cross-Image introduces an *attention contrasting* hyperparameter to promote relevant alignment and suppress noise. One might expect tuning it could fix leakage, but as shown in Figure 2, the issue persists without proper Query-Key alignment. Another strategy is to apply an object *mask* [25], yet leakage can still occur within the masked area. Even with accurate masks, the model often overfits local style rather than ensuring semantic alignment, resulting in unnatural images. We revisit this in the experiments (Figure 6).

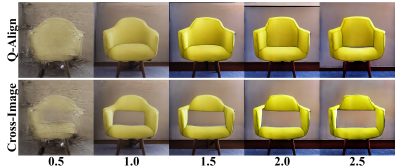


Figure 2: Results of Q-Align (ours) and Cross-Image with varying contrast strength.

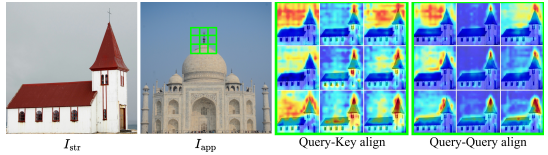


Figure 3: Query-Key vs Query-Query alignment. The right two images present zoomed-in attention maps for the green 3×3 grid in I_{app} .

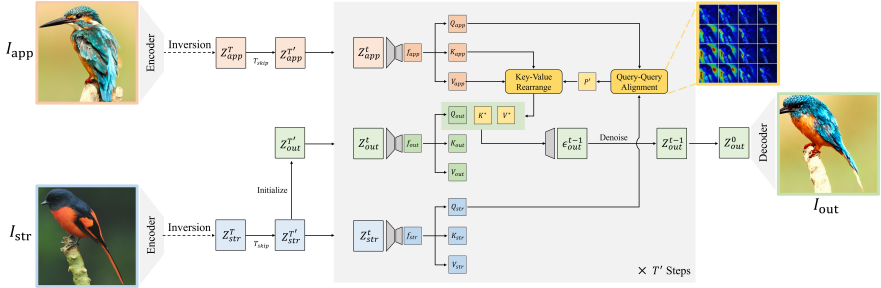


Figure 4: Illustration of Q-Align. We omit the superscript t from Q, K, V for brevity.

4 Q-Align

We propose Q-Align to address misalignment between semantically corresponding regions in the image pair. Specifically, we obtain sophisticated feature mapping between two images based on query-query alignment, and rearrange key and value for better query-key-value correspondence. Lastly, refined attention is created by utilizing the rearranged keys and values, enabling the capture of semantic correspondence between both images. The entire procedure of Q-Align is illustrated in Figure 4.

4.1 Query-Query alignment

The main cause of attention leakage is the feature misalignment in the cross-image attention. To mitigate this, we leverage the *query-query alignment* between Q_{str} and Q_{app} . Since queries determine the semantic meaning of each spatial location in an image, we claim that query-query alignment can provide aligned features between two images more accurately than query-key alignment of Cross-Image. In this paper, we measure the query-query alignment with an alignment matrix S :

$$S = Q_{app} Q_{str}^\top, \quad (2)$$

where $S \in \mathbb{R}^{n \times n}$ and n is the number of queries. Each element $S_{r,c}$ indicates the similarity score between the r -th query of Q_{app} and the c -th query of Q_{str} .

Empirical Evidence. Figure 3 shows that the query-query alignment ($\text{softmax}(Q_{str} Q_{app}^\top)$) achieves better correspondence than query-key alignment ($\text{softmax}(Q_{str} K_{app}^\top)$). The query-query alignment provides more sophisticated spatial attention, while the query-key alignment distributes attention broadly across related regions. For example, for the finial tip in I_{app} (second column in the green grid), query-key alignment distributes attentions to the body

part of the building in I_{str} , while our query-query alignment sharply focuses on the finial tip in I_{str} . Similarly, for the right pitched roof in I_{app} (third column in the green grid), query-key alignment broadly focuses on the background in I_{str} , whereas our query-query alignment precisely attends to the right pitched roof area in I_{str} . Therefore, by leveraging the query-query alignment to extract precise and detailed points of interest, we could enable the model to accurately and comprehensively focus on relevant regions.

4.2 Key-Value Rearrangement

We utilize the query-query alignment S between Q_{str} and Q_{app} to rearrange $(K_{\text{app}}, V_{\text{app}})$ for better query-key-value correspondence, based on our demonstration that S provides precise feature alignment between I_{str} and I_{app} . It is important to recognize that we modify the keys and values rather than the queries, as queries define the semantic meaning of each spatial location in an image. Modifying the queries could potentially disrupt the structural semantics of the output image.

Rearrangement Matrix. Specifically, we construct an aggregation matrix $P \in \mathbb{R}^{n \times n}$ for the key-value rearrangement based on the query-query alignment S , as follows:

$$(P^{\top})_{r,c} = \begin{cases} \frac{1}{k}, & \text{if } S_{r,c} \in \text{Top-}k(S_r) \\ 0, & \text{otherwise} \end{cases} \quad (3)$$

$\text{Top-}k(S_r)$ denotes the set of top- k values in each row $S_r \in \mathbb{R}^n$. It is worth noting that we only retain top- k alignments for key-value rearrangement, as larger k broadens the range of features aggregated and may dilute the distinctiveness of the generated image. In this paper, we use $k = 1$. If the sum of any row in P is 0, we set the diagonal entry to 1 to maintain the original keys/values:

$$P_{r,r} = 1, \text{ If } \sum_{c=1}^n P_{r,c} = 0. \quad (4)$$

We then apply row-wise softmax reweighting to P :

$$P'_{r,c} = \begin{cases} \frac{e^{P_{r,c}}}{\sum_{c' \in [n], P_{r,c'} \neq 0} e^{P_{r,c'}}}, & \text{if } P_{r,c} \neq 0 \\ 0, & \text{if } P_{r,c} = 0 \end{cases} \quad (5)$$

It is noted that we ensure that elements with an initial value of 0 remain unchanged. Each element $P'_{r,c}$ indicates the contribution weights of the c -th feature on the r -th feature.

Key-Value Rearrangement via Aggregation. The aggregation matrix P' is applied to modify the original key matrix K_{app} and the original value matrix V_{app} , to create a rearranged key matrix K^* and value matrix V^* :

$$K^* = P' K_{\text{app}}, \quad (6)$$

$$V^* = P' V_{\text{app}}. \quad (7)$$

For example, if $P'_{10,20} = 1$, the 20th key and value are rearranged to be aligned with the 10th query. By leveraging the query-query alignment to rearrange the key/value matrix, K^* and V^* achieve improved feature alignment with Q_{str} . This alignment extends to Q_{out} used for generating the output image. Consequently, the modified key K^* and the modified value

	Q-Align(ours)	Cross-Image	DragonDiffusion	DiffuseIT	SpliceViT
Gram Loss	2.9 / 3rd	2.5 / 2nd	3.2 / 5th	3.1 / 4th	1.3 / 1st
GPT	4.5 / 1st	4.3 / 2nd	3.9 / 3rd	3.5 / 4th	2.8 / 5th

[Generated Rationale Behind Q-Align Appearance Fidelity Score]

- **Strengths:** The output closely retains the giraffe's color and texture details from the Appearance Image. The overall style matches well, with sharp and clear textures.

- **Weaknesses:** Minor distortions in the left hind leg but does not significantly detract from the overall appearance.

[Generated Rationale Behind Cross-Image Appearance Fidelity Score]

- **Strengths:** Similar to QAlign, it effectively maintains color and texture fidelity, and the overall giraffe shape is well-defined.

- **Weaknesses:** Slight blurring noticed on the back might reduce overall clarity compared to QAlign.

...

Figure 5: Comparison between our GPT-based Appearance Fidelity Score (Table 2) and Gram Loss (Table 1). The example is from Figure 6, and details can be found in the supplementary material.

V^* align their features with the most relevant query vectors, thereby mitigating the issue of attention leakage.

Rearranged Cross-Image Attention Finally, we deploy the rearranged key K^* and value V^* for the Cross-Image attention between I_{out} and I_{app} :

$$\text{softmax} \left(\frac{Q_{\text{out}}(K^*)^\top}{\sqrt{d}} \right) V^*. \quad (8)$$

This formulation maintains semantic consistency during the appearance transfer, ensuring that Q_{out} , K^* , and V^* are aligned correctly while reducing the generation of unintended artifacts.

5 Experiments

5.1 Experiment setting

Datasets. Following Cross-Image [1], we selected *six* domains (animal faces, animals, cars, birds, buildings, and cakes) to enable a fair comparison. As done in Cross-Image [1], for the animal face domain, images from AFHQ [2] were utilized. For the remaining domains, we utilized images from the official Cross-Image page as well as copyright-free real-world images from Unsplash². To ensure diversity in the dataset, we gathered 30 image pairs per domain, resulting in a total of 180 pairs.

Baseline Methods. We compare Q-Align with state-of-the-art approaches, including Cross-Image [1], DragonDiffusion [2], DiffuseIT [13], and SpliceViT [3]. All methods were implemented using the official code provided by the respective authors, following their default parameters. We use Stable Diffusion [28] as the base model, and the same random seed and other processing parameters are applied uniformly. Further details on parameter settings and implementation specifics are provided in the supplementary materials.

²<https://unsplash.com>

Domain	Gram Loss ↓		IoU ↑	
	Cross-Image	Q-Align	Cross-Image	Q-Align
Animal	1.08 / 0.64	1.68 / 1.77	0.66 / 0.16	0.71 / 0.12
Animal Face	0.79 / 0.43	0.84 / 0.42	0.72 / 0.18	0.78 / 0.10
Bird	1.47 / 0.85	1.37 / 0.75	0.75 / 0.15	0.80 / 0.09
Building	4.92 / 4.03	4.68 / 2.38	0.81 / 0.17	0.82 / 0.17
Cake	3.16 / 3.26	2.58 / 2.11	0.78 / 0.23	0.84 / 0.11
Car	1.12 / 0.32	1.32 / 0.35	0.84 / 0.17	0.83 / 0.17
Avg	2.09 / 1.59	2.08 / 1.30	0.76 / 0.18	0.80 / 0.13

Table 1: Mean and standard deviation of Gram Loss and IoU for each domain (Mean / Std).

Appearance Fidelity Score					
Domain	SpliceViT	DiffuseIT	DragonDiffusion	Cross-Image	Q-Align (ours)
Animal	2.54 / 0.51	3.65 / 0.47	3.69 / 0.58	4.04 / 0.50	4.25 / 0.41
Animal Face	2.49 / 0.58	3.41 / 0.39	3.72 / 0.53	4.29 / 0.28	4.31 / 0.30
Bird	2.68 / 0.39	3.36 / 0.48	3.88 / 0.53	4.15 / 0.29	4.31 / 0.19
Building	2.16 / 0.50	3.20 / 0.39	3.52 / 0.35	4.36 / 0.14	4.46 / 0.17
Cake	2.56 / 0.64	2.93 / 0.49	4.15 / 0.51	4.09 / 0.42	4.23 / 0.32
Car	2.23 / 0.40	3.21 / 0.40	3.86 / 0.41	4.22 / 0.36	4.21 / 0.42
Avg	2.44 / 0.54	3.29 / 0.49	3.80 / 0.53	4.19 / 0.37	4.30 / 0.33

Table 2: GPT-based appearance fidelity score across different methods (Mean/Std).

Structural Consistency Score					
Domain	SpliceViT	DiffuseIT	DragonDiffusion	Cross-Image	Q-Align (ours)
Animal	2.66 / 0.50	3.77 / 0.57	3.76 / 0.71	3.93 / 0.57	4.17 / 0.46
Animal Face	2.54 / 0.50	3.42 / 0.30	3.73 / 0.55	4.35 / 0.29	4.41 / 0.22
Bird	2.81 / 0.51	3.41 / 0.48	4.00 / 0.58	4.08 / 0.42	4.21 / 0.34
Building	2.31 / 0.55	3.23 / 0.41	3.42 / 0.48	4.41 / 0.19	4.50 / 0.14
Cake	2.85 / 0.67	3.02 / 0.63	4.26 / 0.57	4.15 / 0.36	4.24 / 0.29
Car	2.34 / 0.34	3.28 / 0.38	4.07 / 0.44	4.33 / 0.22	4.32 / 0.29
Avg	2.58 / 0.56	3.35 / 0.53	3.87 / 0.62	4.21 / 0.40	4.31 / 0.33

Table 3: GPT-based structural consistency score across different methods (Mean/Std).

Evaluation Metrics (existing). In the earlier work [10], they used Gram loss [8] computed on VGG-19 features [20] for the appearance fidelity, and IoU between object masks [16] of I_{out} and I_{str} for the structural consistency. However, as shown in Table 1, applying those evaluation metrics proposed in Cross-Image led to significant variance across different samples, which limited the reliability of the quantitative assessment. Furthermore, Figure 5 shows that the appearance similarity perceived by humans does not align well with the results of the Gram loss metric.

GPT-based Metrics (proposed). To address these limitations, we propose a novel evaluation protocol leveraging GPT-4o series [15]³, a powerful large language model with a vision capability. Inspired by [22], we prompt GPT with a detailed explanation of the appearance transfer task and explicitly defined two evaluation criteria (*i.e.*, appearance fidelity and structural consistency). We then instruct GPT to rate each criterion on a scale from 1.0 to 5.0. A comprehensive description of the prompt design is provided in the supplementary material. As shown in Figure 5, GPT assigns scores at a level comparable to human evaluation while also providing explanations for its reasoning.

5.2 Experiment results

Quantitative Comparison. Table 2 and Table 3 present the quantitative evaluation of appearance transfer across different methods, based on the proposed GPT-based appearance fidelity and structural consistency scores. In terms of appearance, Q-Align achieved the best results in most domains, with the highest average score. In terms of structure, Q-Align also achieved the highest average structural consistency score, surpassing other methods by notable margins. By addressing the attention leakage issue and preventing unnecessary artifacts, Q-Align achieved both strong structure preservation and high appearance similarity, indicating that it delivered the best overall results for the appearance transfer task.

Qualitative Results. Figure 6 presents a comparison of appearance transfer results across different models, highlighting the distinct advantages of Q-Align. DragonDiffusion showed vibrant color but produced distorted images. As a mask-based approach, it prioritized fitting the style within the mask region rather than ensuring accurate semantic mapping. For instance, in the building example, the appearance image contained rounded roofs, meaning

³we use gpt-4o-mini-2024-07-18 with OpenAI API



Figure 6: Qualitative comparison across different methods. Each row displays an example consisting of the structure image, appearance image, and the outputs from our method, Cross-Image, DragonDiffusion, DiffuseIT, and SpliceViT. For demonstration purposes, we select samples that exhibit attention leakage in Cross-Image. More qualitative results are presented in the supplementary materials.

that the appearance transfer output should exhibit a rounded roof shape. However, DragonDiffusion forced the style into the original pointed roof mask, resulting in an unnatural composition. Cross-Image exhibited attention leakage, where objects appeared in the background, background elements were incorrectly mapped onto objects, or incorrect semantic mappings occurred within both object and background regions. For example, in the bird image, wing characteristics appeared in the background, and in the vehicle image, bumper traits (e.g., gray tones) were mapped onto the doors. Additionally, in the animal category, the background color was incorrectly mapped. In contrast, Q-Align demonstrated reliable performance in preserving both structural and appearance features, consistently generating high-quality and faithful appearance transfer results across diverse examples.

5.3 Study on Q-Align

Figure 7 shows the appearance transfer results of Cross-Image and Q-Align. We first observe that Cross-Image generates an undesirable image of a chair. A clue for this issue can be found in the Query-Key alignment, where the background is incorrectly aligned to the center of the chair. As a result, Cross-Image generates a background-colored hole in the

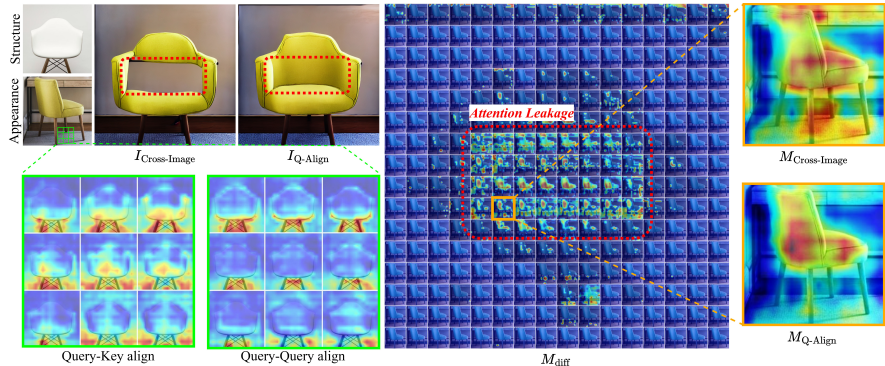


Figure 7: Zero-shot appearance transfer with Cross-Image and Q-Align. We present Query-Key alignment and Query-Query alignment for the 3×3 green grid. $M_{\text{diff}} = |M_{\text{Cross-Image}} - M_{\text{Q-Align}}|$ represents attention difference. Values below 0.2 are masked as 0 to emphasize only significant differences.

chair. Query-Query alignment, on the other hand, prevents any attention leakage from the background onto the chair. The attention difference map M_{diff} highlights areas with significant differences in semantic focus, emphasizing central regions where attention leakage occurs in Cross-Image. We observe that, when generating the center of the chair, Cross-Image attends to both the chair and the background, whereas Q-Align focuses solely on the chair itself. This result aligns with Zhang et al. [89], who highlighted that queries and keys reside in distinct embedding spaces. We assert that query-query alignment, occurring within the same embedding space, inherently achieves better alignment than query-key alignment.

6 Related Work

Semantic Alignment. Most studies have focused on learning semantic correspondences between images through supervised training [8, 19, 31, 32]. While these approaches demonstrate high performance, they come with the limitation of requiring large-scale datasets. To address this, methods that utilize features from pre-trained vision transformers [1, 8, 11] have been proposed, along with the image manipulation methodologies [18, 33]. More recent approaches utilize large-scale image generation models [11, 21, 28] to extract features that enable precise semantic mapping between images [13, 24, 30, 38]. Additionally, controlling the attention map of large models for manipulation has been explored [3, 14, 26, 32], enabling semantic coherence to be preserved without the need for additional training.

Attention in Diffusion Models. Attention mechanisms [35] are fundamental in diffusion-based image manipulation, with numerous studies focused on optimizing [36], modifying [3, 14, 17, 26, 37], and refining [1, 21]. Among these, methods that mix the query of one image with the key and value of another have been developed to support non-rigid image editing [3, 17, 37]. Other studies utilize refined attention masks to guide the accurate designation of regions for modification within an image [1, 21], while some employ latent optimization to prevent focusing on irrelevant regions [38]. In this study, we propose a zero-shot method that operates without any external masks or additional optimization, relying solely on query-query alignment. This design effectively mitigates attention leakage while

preserving both structural consistency and semantic fidelity unlike mask-based approaches that distort semantics by forcing styles into fixed mask regions.

7 Conclusion

We proposed Q-Align, a novel method that utilizes Query-Query alignment to effectively rearrange keys and values for the attention mechanism. Our method offers a zero-shot, straightforward solution that directly addresses the critical issue of attention leakage observed in SOTA methods. Through comprehensive analysis and extensive experiments, we demonstrated that Q-Align not only effectively resolves attention leakage but also significantly outperforms existing approaches. As future work, we envision extending Q-Align to incorporate fine-grained semantic mapping techniques, which we expect will further enhance its capability for precise and high-quality appearance transfer.

Acknowledgments

This work was supported by the Digital Innovation Hub project supervised by the Daegu Digital Innovation Promotion Agency (DIP), grant funded by the Korea government (MSIT and Daegu Metropolitan City) in 2025 (No. 25DIH-11, Development of Model Context Protocol (MCP)-Based Multi-Agent Collaborative System for Large Language Models (LLMs)).

※ MSIT: Ministry of Science and ICT.

References

- [1] Yuval Alaluf, Daniel Garibi, Or Patashnik, Hadar Averbuch-Elor, and Daniel Cohen-Or. Cross-image attention for zero-shot appearance transfer. In *SIGGRAPH*, 2024.
- [2] Herbert Bay, Tinne Tuytelaars, and Luc Van Gool. Surf: Speeded up robust features. In *ECCV*, 2006.
- [3] Mingdeng Cao, Xintao Wang, Zhongang Qi, Ying Shan, Xiaohu Qie, and Yinqiang Zheng. Masactr: Tuning-free mutual self-attention control for consistent image synthesis and editing. In *ICCV*, 2023.
- [4] Mathilde Caron, Hugo Touvron, Ishan Misra, Hervé Jégou, Julien Mairal, Piotr Bojanowski, and Armand Joulin. Emerging properties in self-supervised vision transformers. In *ICCV*, 2021.
- [5] Seokju Cho, Sunghwan Hong, and Seungryong Kim. Cats++: Boosting cost aggregation with convolutions and transformers. *IEEE TPAMI*, 2023.
- [6] Yunjey Choi, Youngjung Uh, Jaejun Yoo, and Jung-Woo Ha. Stargan v2: Diverse image synthesis for multiple domains. In *CVPR*, 2020.
- [7] Guillaume Couairon, Jakob Verbeek, Holger Schwenk, and Matthieu Cord. Diffedit: Diffusion-based semantic image editing with mask guidance. In *ICLR*, 2023.

- [8] Alexey Dosovitskiy, Lucas Beyer, Alexander Kolesnikov, Dirk Weissenborn, Xiaohua Zhai, Thomas Unterthiner, Mostafa Dehghani, Matthias Minderer, Georg Heigold, Sylvain Gelly, Jakob Uszkoreit, and Neil Houlsby. An image is worth 16x16 words: Transformers for image recognition at scale. In *ICLR*, 2021.
- [9] Leon A. Gatys, Alexander S. Ecker, and Matthias Bethge. A neural algorithm of artistic style. *arXiv preprint arXiv:1508.06576*, 2015.
- [10] Shuyang Gu, Dong Chen, Jianmin Bao, Fang Wen, Bo Zhang, Dongdong Chen, Lu Yuan, and Baining Guo. Vector quantized diffusion model for text-to-image synthesis. In *CVPR*, 2022.
- [11] Kamal Gupta, Varun Jampani, Carlos Esteves, Abhinav Shrivastava, Ameesh Makadia, Noah Snavely, and Abhishek Kar. Asic: Aligning sparse in-the-wild image collections. In *ICCV*, 2023.
- [12] Mark Hamilton, Zhou Tong Zhang, Bharath Hariharan, Noah Snavely, and William T. Freeman. Unsupervised semantic segmentation by distilling feature correspondences. In *ICLR*, 2022.
- [13] Eric Hedlin, Gopal Sharma, Shweta Mahajan, Hossam Isack, Abhishek Kar, Andrea Tagliasacchi, and Kwang Moo Yi. Unsupervised semantic correspondence using stable diffusion. In *NeurIPS*, 2023.
- [14] Amir Hertz, Ron Mokady, Jay Tenenbaum, Kfir Aberman, Yael Pritch, and Daniel Cohen-Or. Prompt-to-prompt image editing with cross attention control. In *ICLR*, 2023.
- [15] Aaron Hurst, Adam Lerer, Adam P Goucher, Adam Perelman, Aditya Ramesh, Aidan Clark, AJ Ostrow, Akila Welihinda, Alan Hayes, Alec Radford, et al. Gpt-4o system card. *arXiv preprint arXiv:2410.21276*, 2024.
- [16] Lei Ke, Mingqiao Ye, Martin Danelljan, Yifan Liu, Yu-Wing Tai, Chi-Keung Tang, and Fisher Yu. Segment anything in high quality. In *NeurIPS*, 2023.
- [17] Gwanhyeong Koo, Sunjae Yoon, Ji Woo Hong, and Chang D Yoo. Flexiedit: Frequency-aware latent refinement for enhanced non-rigid editing. *arXiv preprint arXiv:2407.17850*, 2024.
- [18] Gihyun Kwon and Jong Chul Ye. Diffusion-based image translation using disentangled style and content representation. In *ICLR*, 2023.
- [19] Jae Yong Lee, Joseph DeGol, Victor Fragoso, and Sudipta N. Sinha. Patchmatch-based neighborhood consensus for semantic correspondence. In *CVPR*, 2021.
- [20] Shanglin Li, Bohan Zeng, Yutang Feng, Sicheng Gao, Xiupei Liu, Jiaming Liu, Lin Li, Xu Tang, Yao Hu, Jianzhuang Liu, and Baochang Zhang. Zone: Zero-shot instruction-guided local editing. In *CVPR*, 2024.
- [21] Bingyan Liu, Chengyu Wang, Tingfeng Cao, Kui Jia, and Jun Huang. Towards understanding cross and self-attention in stable diffusion for text-guided image editing. In *CVPR*, 2024.

- [22] Yang Liu, Dan Iter, Yichong Xu, Shuohang Wang, Ruochen Xu, and Chenguang Zhu. G-eval: NLG evaluation using gpt-4 with better human alignment. In *ACL*, 2023.
- [23] DG Lowe. Distinctive image features from scale-invariant key points. *Int. J. Comput. Vis.*, 2004.
- [24] Grace Luo, Lisa Dunlap, Dong Huk Park, Aleksander Holynski, and Trevor Darrell. Diffusion hyperfeatures: Searching through time and space for semantic correspondence. In *NeurIPS*, 2023.
- [25] Chong Mou, Xintao Wang, Jiechong Song, Ying Shan, and Jian Zhang. Dragondiffusion: Enabling drag-style manipulation on diffusion models. In *ICLR*, 2024.
- [26] Gaurav Parmar, Krishna Kumar Singh, Richard Zhang, Yijun Li, Jingwan Lu, and Jun-Yan Zhu. Zero-shot image-to-image translation. In *SIGGRAPH*, 2023.
- [27] Aditya Ramesh, Prafulla Dhariwal, Alex Nichol, Casey Chu, and Mark Chen. Hierarchical text-conditional image generation with clip latents. *arXiv preprint arXiv:2204.06125*, 2022.
- [28] Robin Rombach, Andreas Blattmann, Dominik Lorenz, Patrick Esser, and Björn Ommer. High-resolution image synthesis with latent diffusion models. In *CVPR*, 2022.
- [29] Karen Simonyan and Andrew Zisserman. Very deep convolutional networks for large-scale image recognition. *arXiv preprint arXiv:1409.1556*, 2015.
- [30] Luming Tang, Menglin Jia, Qianqian Wang, Cheng Perng Phoo, and Bharath Hariharan. Emergent correspondence from image diffusion. In *NeurIPS*, 2023.
- [31] Zachary Teed and Jia Deng. Raft: Recurrent all-pairs field transforms for optical flow. In *ECCV*, 2020.
- [32] Prune Truong, Martin Danelljan, Luc V Gool, and Radu Timofte. Gocor: Bringing globally optimized correspondence volumes into your neural network. In *NeurIPS*, 2020.
- [33] Narek Tumanyan, Omer Bar-Tal, Shai Bagon, and Tali Dekel. Splicing vit features for semantic appearance transfer. In *CVPR*, 2022.
- [34] Narek Tumanyan, Michal Geyer, Shai Bagon, and Tali Dekel. Plug-and-play diffusion features for text-driven image-to-image translation. In *CVPR*, 2023.
- [35] Ashish Vaswani, Noam Shazeer, Niki Parmar, Jakob Uszkoreit, Llion Jones, Aidan N Gomez, Łukasz Kaiser, and Illia Polosukhin. Attention is all you need. In *NeurIPS*, 2017.
- [36] Kai Wang, Fei Yang, Shiqi Yang, Muhammad Atif Butt, and Joost van de Weijer. Dynamic prompt learning: Addressing cross-attention leakage for text-based image editing. In *NeurIPS*, 2023.
- [37] Sihan Xu, Yidong Huang, Jiayi Pan, Ziqiao Ma, and Joyce Chai. Inversion-free image editing with language-guided diffusion models. In *CVPR*, 2024.

- [38] Junyi Zhang, Charles Herrmann, Junhwa Hur, Luisa Polania Cabrera, Varun Jampani, Deqing Sun, and Ming-Hsuan Yang. A tale of two features: Stable diffusion complements dino for zero-shot semantic correspondence. In *NeurIPS*, 2023.
- [39] Shujian Zhang, XINJIE FAN, Huangjie Zheng, Korawat Tanwisuth, and Mingyuan Zhou. Alignment attention by matching key and query distributions. In *NeurIPS*, 2021.